AGU PUBLICATIONS

JGR

Journal of Geophysical Research: Space Physics

RESEARCH ARTICLE
10.1002/2017JA024565

Key Points:
- We present the spatial distribution of plasma sheet temperature and density in GSM *X-Y* plane using 21 years of in situ Geotail data
- Cold-dense plasma sheet occurrence rates have a semiannual variation, in keeping with the semiannual variation of the IMF + B_z
- The Russell-McPherron effect may therefore control these variations and hence modulate solar wind entry into the magnetosphere

Supporting Information:
- Supporting Information S1
- Figure S1
- Figure S2

Correspondence to:
Q. Shi and M. Nowada,
sqq@pku.edu.cn;
moto.nowada@sdu.edu.cn

Citation:
Bai, S., Shi, Q., Tian, A., Nowada, M., Degeling, A. W., Zhou, X.-Z., … Fazakerly, A. N. (2018). Spatial distribution and semiannual variation of cold-dense plasma sheet. *Journal of Geophysical Research: Space Physics*, *123*, 464–472. https://doi.org/10.1002/2017JA024565

Received 14 JUL 2017
Accepted 29 DEC 2017
Accepted article online 5 JAN 2018
Published online 23 JAN 2018

Spatial Distribution and Semiannual Variation of Cold-Dense Plasma Sheet

Shichen Bai[1,2], Quanqi Shi[1], Anmin Tian[1], Motoharu Nowada[1], Alexander W. Degeling[1], Xu-Zhi Zhou[3], Qiu-Gang Zong[3], I. Jonathan Rae[5], Suiyan Fu[3], Hui Zhang[4], Zuyin Pu[3], and Andrew N. Fazakerly[5]

[1]Shandong Provincial Key Laboratory of Optical Astronomy and Solar-Terrestrial Environment, School of Space Science and Physics, Shandong University, Weihai, China, [2]State Key Laboratory of Space Weather, National Space Science Center, Chinese Academy of Sciences, Beijing, China, [3]School of Earth and Space Sciences, Peking University, Beijing, China, [4]Physics Department and Geophysical Institute, University of Alaska Fairbanks, Fairbanks, AK, USA, [5]Mullard Space Science Laboratory, Department of Space and Climate Physics, University College London, Dorking, UK

Abstract The cold-dense plasma sheet (CDPS) plays an important role in the entry process of the solar wind plasma into the magnetosphere. Investigating the seasonal variation of CDPS occurrences will help us better understand the long-term variation of plasma exchange between the solar wind and magnetosphere, but any seasonal variation of CDPS occurrences has not yet been reported in the literature. In this paper, we investigate the seasonal variation of the occurrence rate of CDPS using Geotail data from 1996 to 2015 and find a semiannual variation of the CDPS occurrences. Given the higher probability of solar wind entry under stronger northward interplanetary magnetic field (IMF) conditions, 20 years of IMF data (1996–2015) are used to investigate the seasonal variation of IMF B_z under northward IMF conditions. We find a semiannual variation of IMF B_z, which is consistent with the Russell-McPherron (R-M) effect. We therefore suggest that the semiannual variation of CDPS may be related to the R-M effect.

1. Introduction

The formation of the cold-dense plasma sheet (CDPS) is considered a representative signature of solar wind entry under northward interplanetary magnetic field (IMF) conditions seen in the magnetosphere (e.g., Fujimoto et al., 1996; Stenuit et al., 2002; Terasawa et al., 1997; Wing & Newell, 2002). CDPS is generally characterized by high density ($n > 1$ cm^{-3}) and low temperature ($T < 2$ keV) with a low ion bulk flow speed ($|V_x| < 100$ km/s) (e.g., Baumjohann et al., 1989; Fujimoto et al., 1996, 2002; Li et al., 2005; Wing, Johnson, & Fujimoto, 2006). Observations have shown that a cold-dense plasma sheet forms after a long duration of northward IMF (e.g., Terasawa et al., 1997; Wing et al., 2005). A cold and dense plasma sheet can also be considered as a precondition for the strong ring current that forms during geomagnetic storms (Thomsen et al., 2003; Lavraud, Thomsen, Borovsky, et al., 2006; Chen et al., 2007) and also affects magnetosphere-ionosphere coupling (e.g., Gkioulidou et al., 2009). The magnetospheric flank regions are believed to be the source region of the CDPS. Plasmas with low temperature and high density in the flank region are source components of CDPS, provided by the solar wind entry during the northward IMF period. Double-lobe reconnection (Crooker, 1992; Fuselier et al. 2002; Lavraud, Thomsen, Lefebvre, et al., 2006; Le et al., 1996; Li et al., 2008; Onsager et al., 2001; Sandholt et al., 1999; Song & Russell, 1992; Shi et al., 2009, 2013) could be an important mechanism to transport cold and dense plasma from solar wind to the magnetosphere. Lavraud et al. (2005) found evidence of double-lobe reconnection at high latitudes. Shi et al. (2013) found a new region of solar wind plasma entry into the magnetosphere, in the lobes tailward of the cusp, and lobe reconnection was suggested to be the most probable mechanism of the entry. Based on OpenGGCM MHD simulations, Li et al. (2005) simulated the process of cold-dense plasma sheet transport from the solar wind into the magnetosphere through dual-lobe reconnection. The Kelvin-Helmholtz (K-H) instability in the magnetospheric flank regions is another mechanism for solar wind entry under northward IMF conditions (e.g., Fairfield et al., 2000; Fujimoto, Tonooka, & Mukai, 2003; Hasegawa et al., 2004, 2009; Miura, 1987). Other mechanisms such as impulsive penetration (e.g., Echim & Lemaire, 2002) and gradient drift (e.g., Olson & Pfitzer, 1985; Zhou et al., 2007) may also play a role in the plasma interchange between the solar wind and magnetosphere under northward IMF conditions.

Previous works mainly focus on the formation and transport mechanisms of CDPS (e.g., Fujimoto, Mukai, & Kokubun, 2002; Nishino et al., 2007a, 2007b, Nishino, Fujimoto, Ueno, et al., 2007, Nishino, Fujimoto, Ueno,

Mukai, et al., 2007; Wang et al., 2014; Wing et al., 2006). However, the seasonal variation of the CDPS occurrence has not been studied. Through the investigation of seasonal variation of the CDPS occurrence, we gain a basic understanding of the seasonal variation of the mass interchange rate between the solar wind and magnetosphere during quiet times.

Since the CDPS particle source has been considered to be from the solar wind, the variation of solar wind conditions should control the variation of CDPS occurrence. The semiannual variation of geomagnetic activity has been reported for over a hundred years (Sabine, 1851). Several hypotheses were proposed to explain this variation, such as the axial hypothesis (Cortie, 1912; Svalgaard, 1977), the equinoctial hypothesis (Bartels, 1932; Cliver et al., 2002, 2000; McIntosh, 1959) and the Russell-McPherron (R-M) effect (Russell & McPherron, 1973). The axial hypothesis attributes the semiannual variation to the variation of the Earth's heliographic latitude. During March and September the heliographic latitude of Earth approaches the range of values where sunspots appear frequently and the average solar wind velocity is higher (Hundhausen et al., 1971). The equinoctial hypothesis considers the φ angle between the Earth-Sun line and the dipole axis of the Earth as the key parameter that affects the field configuration in the Chapman-Ferraro current plane (Crooker & Siscoe, 1986). This suppresses the transfer of energy and further influences the coupling efficiency between solar wind and magnetosphere. The R-M effect proposes that the θ angle is a key parameter, which is defined as the angle between Y axis in geocentric solar equatorial (GSE) coordinate and Z axis in geocentric solar magnetospheric (GSM) coordinates, when examining components of the IMF. According to the R-M effect, the instantaneous IMF-Z_{GSM} component increases in association with a decrease of the angle θ, whose range is smaller than 90°. The minimum of θ appears at spring and fall equinoxes. The maximum of angle θ is seen at summer and winter solstices, when the GSE B_y projection effect minimizes and the magnitude of GSM B_z reaches its maximum. Previous studies on R-M effect focused on understanding the role of R-M effect for southward IMF conditions (e.g., O'Brien & McPherron, 2002; Russell & McPherron, 1973; Siscoe & Crooker, 1996; Zhao & Zong, 2012) and for the dipole effect under various IMF orientations (Nowada et al., 2009; Russell, Wang, & Raeder, 2003), while no attempts have been made under northward IMF. However, several works have suggested the higher occurrence of solar wind entry with stronger northward IMF (Lavraud, Thomsen, Lefebvre, et al., 2006; Lin et al., 2014; Zhou et al., 2007). Therefore, in this paper, we investigate the seasonal variation of CDPS occurrences and the possible role that the R-M effect plays in the seasonal variation of northward IMF, and then build a possible link between the R-M effect and the CDPS occurrences.

2. Observations

2.1. Data Set

The CDPS events are identified by use of the magnetic field (MGF) experiment data (Kokubun et al., 1994) and the ion moment data in EA modes from the Low-Energy Particle (LEP) experiment with a covered energy range of 60 eV–40 keV (Mukai et al., 1994) and Comprehensive Plasma Instrumentation (CPI) onboard Geotail, with a covered energy range of 1.3 eV–48.2 keV (Frank et al., 1994) from 1996 to 2015. All the results are presented in GSM coordinates.

To investigate the seasonal variation of the northward IMF, IMF data with 1 h time resolution between 1996 and 2015 are used from the OMNI database. The OMNI 1 min resolution data are also used when we calculate the magnetopause location using the Shue et al. (1998) model.

2.2. Cold-Dense Plasma Sheet Observation

All our cases were found in the magnetosphere with the range of $X_{GSM} < -10\ R_E$. To avoid the crossing events of the magnetosheath and low-latitude boundary layer, we only consider the plasma sheet (PS) and cold-dense plasma sheet (CDPS) events, whose radial distance is 3 R_E away from the magnetopause location. The magnetopause location is calculated by Shue et al. (1998) model.

The satellite's traversal of the PS is defined by a sign change of the B_{x_GSM} component. The background flow velocity ($|V_x|$), in the 5 min interval around the time when the spacecraft crosses the center of plasma sheet, should be slower than 100 km/s to avoid the contamination of the magnetosheath. To avoid counting multiple times on the same plasma sheet caused by the flapping motion of magnetotail, and considering the timescale of PS and magnetotail flapping motions, multiple PS crossing points are counted as a single event, if the time interval between two crossings is shorter than 10 min (Sharma et al., 2008). The start time and end time

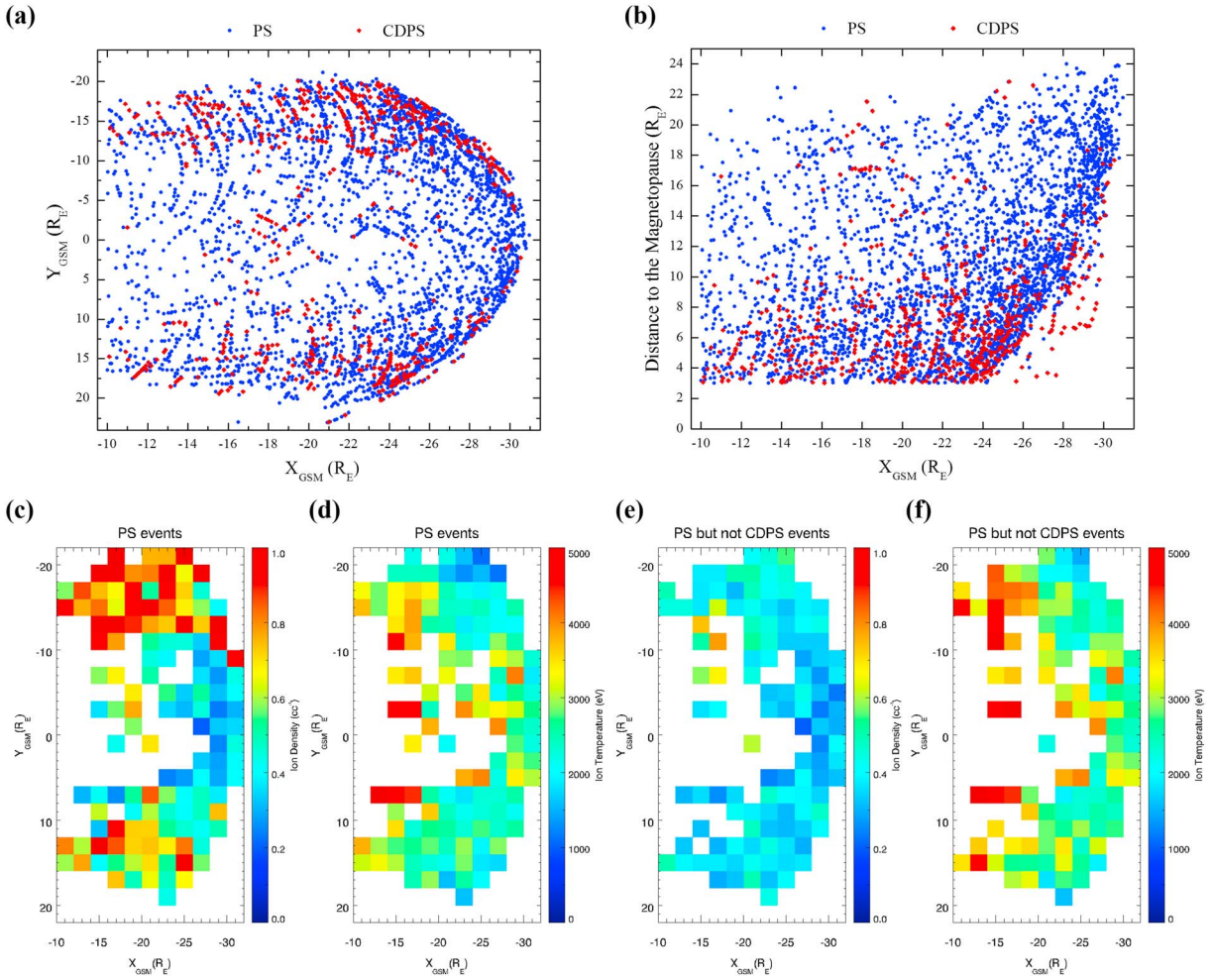

Figure 1. The position of CDPS events (red dots) and PS events (blue dots). The horizontal axis is position of these events in X_{GSM} direction, (a) the *Y* axis is the position in Y_{GSM} direction, and (b) the *Y* axis is the radial distance to the magnetopause. Spatial distribution of (c) ion number density of all plasma sheet crossings events, (d) ion temperature of all plasma sheet crossings events, (e) ion number density of plasma sheet but not cold-dense plasma sheet crossing events, and (f) ion temperature of plasma sheet but not cold-dense plasma sheet crossing events. All observational event points are averaged over 2 $R_E \times 2$ R_E bins. Some regions are left blank because of insufficient data points.

of a single event are determined by the time of the first and last PS crossing points of the PS event. The CDPS events are defined as those PS events that have high ion densities ($N_{ion} > 1$ cc^{-1}) and low ion temperatures ($T_{ion} < 2$ keV) (Fujimoto et al., 1996, 2002), and these two criteria were used for both LEP and CPI data. The plasma parameters data are taken from the LEP instrument when the events are observed by both LEP and CPI. We have not examined the consistency of the two kinds of data. However, for the events that were observed by both instruments, the ion density is close to each other, and the temperature observed by CPI is higher than the LEP value.

Based on the criteria of the PS and CDPS crossings, we identified 636 CDPS events out of 3,770 plasma sheet crossing events. The occurrence rate of CDPS on the duskside is 15.29% and 18.20% on the dawnside, in which the occurrence rate is calculated only using the events on the corresponding side of magnetosphere. The locations of the PS (blue dots) and the CDPS crossing events (red dots), projected onto the GSM *X-Y* plane, are shown in Figure 1 (see Figure S1 in the supporting information for the detailed ion density and temperature of the PS and CDPS events, and the plasma Beta for PS events can be found in Figure S2). Wing & Newell, (2002) showed the projected spatial distribution of ion density and temperature of the plasma sheet from observations in the ionosphere and found a clear dawn-dusk asymmetry in both ion density and ion temperature in the inner magnetosphere. We also investigate the spatial distribution of ion density and temperature based on in situ observations. The spatial distribution of ion number density and temperature of

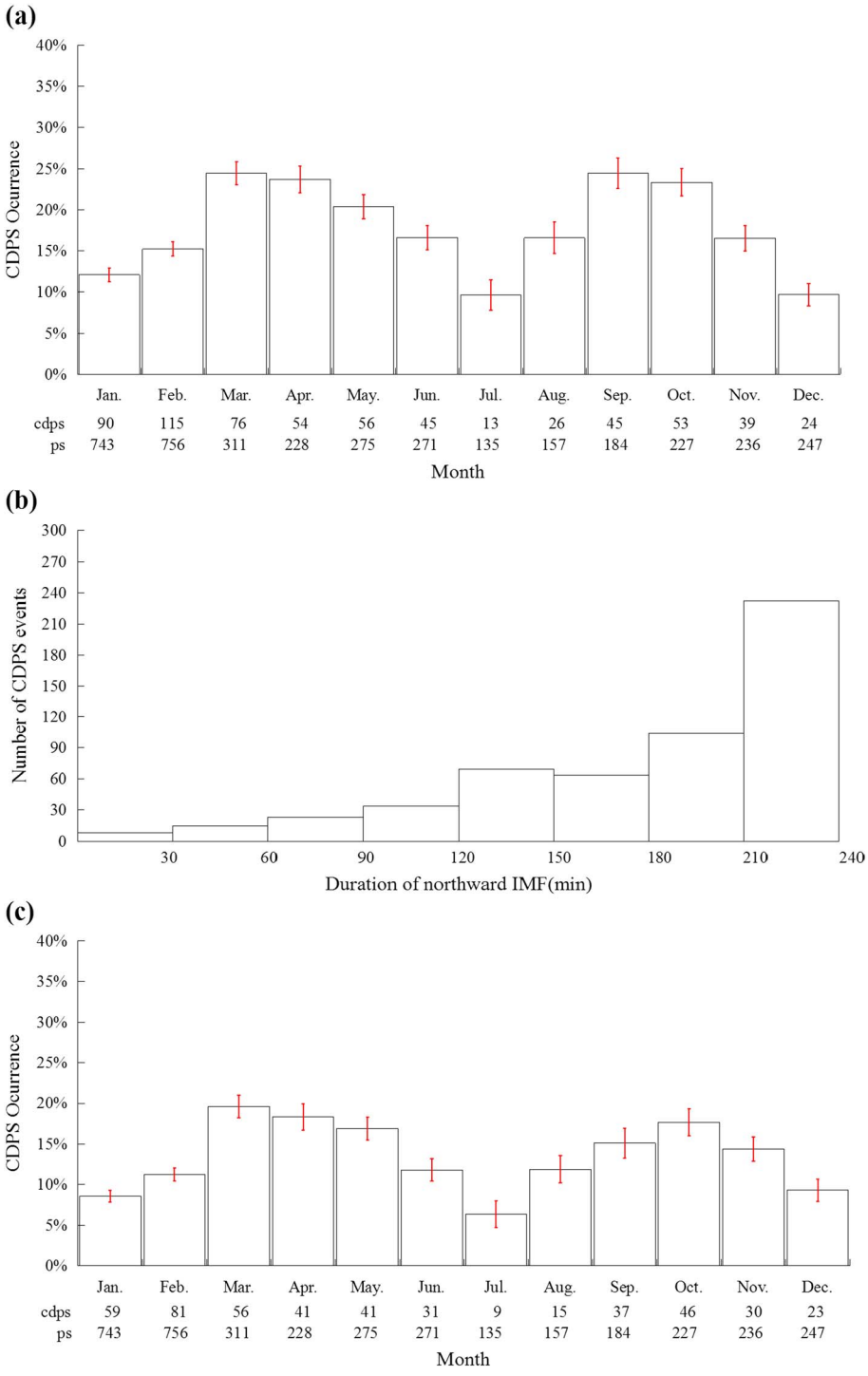

Figure 2. (a) The occurrence rate of CDPS in every month. (b) The number of CDPS events versus the duration of the northward IMF before the observation of CDPS events. (c) The occurrence rate of CDPS in every month that is calculated only using the events with the long period (more than 2 h) of northward IMF before CDPS observation. The CDPS/PS event number in every month is shown at the bottom of Figures 2a and 2c.

PS events projected onto the GSM *X-Y* plane using average values in each 2 $R_E \times 2$ R_E bin are shown in Figures 1c and 1d, respectively. Figures 1e and 1f also show the spatial distribution of ion number density and ion temperature for PS events. Note that CDPS events are excluded from the PS events used to calculate the average values shown in Figures 1e and 1f. There is a clear dawn-dusk asymmetry of average ion density for PS events shown in Figure 1c; however, the difference in average ion temperature for

plasma sheet crossing events in both flanks is not significant, as seen in Figure 1d. The dawn-dusk asymmetry of ion density is not seen in Figure 1e, which indicates that this asymmetry is brought by the CDPS events. The spatial distribution of the ion temperature with or without CDPS is quite similar shown in Figures 1d and 1f, and there is no significant dawn-dusk asymmetry. The number of CDPS/PS events in every month is given in Figure 2a. To examine the seasonal variation of the CDPS occurrence rate, we divided the number of CDPS events in every month by counting the monthly total number of PS events. The result is given in Figure 2a with error bars. The error bar is calculated using the propagation of error analysis and shows below,

$$\Delta N_0 = N_0\left(\frac{\sqrt{n}}{n} - \frac{\sqrt{N}}{N}\right) \quad (1)$$

where n is the number of CDPS events and N is the number of PS events in every month. It seems likely that the CDPS occurrence has a semiannual variation with peaks at March and September and valleys at January and July. Borovsky, Thomsen, and Elphic (1998) reported that it took ~4 h for the solar wind plasma to reach the nightside plasma sheet at geosynchronous orbit. Since the CDPS events we found are outside of geosynchronous orbit, here we investigate the solar wind conditions during a 4 h interval preceding the start of these events. We find that 87 CDPS events are excluded due to the lack of data in this 4 h interval, which leaves 549 events remaining. Figure 2b shows the distribution of the CDPS events as a function of the duration of northward IMF prior to the CDPS event start time. The IMF data are shifted to the CDPS position; the time shift is calculated by X/V_{sw}, where X is the upstream distance of the spacecraft which monitored the IMF and V_{sw} is the measured solar wind speed. The duration in Figure 2b is the sum of the northward IMF periods of time during 4 h before CDPS events. More than 85% (469 out of 549) of the CDPS events experienced at least 2 h of northward IMF within the previous 4 h. This is consistent with previous observations (e.g., Terasawa et al., 1997; Wing et al., 2005). Using these 85% of the CDPS events with at least 2 h of northward IMF prior to the CDPS event and the PS events shown in Figure 2a, we recalculated the CDPS occurrence rate, as shown in Figure 2c. The tendency that CDPS occurrences increased during March and September/October and dropped during January and July remains clear. We also found that most of the CDPS events in our study are during quiet times ($Kp < 3$ and $AE < 150$ nT; see Figure S2); therefore, the semiannual variation of CDPS occurrence should not be related to solar wind entry under southward IMF conditions prior to the identified events.

2.3. Observation of the Northward IMF Variations

It is suggested that the formation of cold-dense plasma sheet requires a long duration of northward IMF (e.g., Terasawa et al., 1997; Wing et al., 2005). Here we use the OMNI 1 h resolution data from 1996 to 2015 to investigate the seasonal variation of the magnitude of the northward IMF (GSM $B_z > 0$) conditions.

Figure 3 shows the seasonal (horizontal axis) and diurnal (vertical axis) variations of northward IMF data calculated on a grid of 24 × 24 bins (with 1 h × 15.25 days for a single bin) and smoothed by a 3 × 3 average. We only use solar wind data during northward IMF periods to calculate the result shown in Figure 3. Figures 3a shows the color contour maps for the probabilities of IMF B_z component larger than 2 nT, and Figure 3b shows the average values of IMF B_z. There are three main assumptions in the R-M effect: (i) the direction of IMF is always along the Parker spiral and its magnitude is constant; (ii) the possibility of meeting southward or northward IMF is equal; and (iii) the northward IMF has no effect on the geomagnetic activity. The R-M effect is put forward to explain the semiannual variation of geomagnetic activities after the solar wind entry under the southward IMF, such as geomagnetic storms and substorms, but the increased magnitude of B_z caused by the projection of GSE B_y could also be expected under northward IMF. The first and second hypotheses are used in this paper. Figure 3c shows the semiannual and diurnal variations of the angle θ under northward IMF conditions, which is the controlling parameter of the R-M effect. Figure 3d shows the semiannual and diurnal variations of the angle φ, which is considered as the key parameter of the equinoctial hypothesis. The peaks of the northward IMF probability are seen between 21:00 UT and 02:00 UT at spring equinox and around 10:00 UT at fall equinox. The valleys of the northward IMF probability existed at summer and winter solstices, and the θ angle reaches a minimum at the same time. The φ angle reaches a minimum at summer and winter solstices, but there is no clear peak or valley of IMF B_z at this time shown in Figures 3a and 3b. The correlation coefficients between Figures 3a and 3b and the two hypotheses shown in Figures 3c and 3d are given in Table 1. The correlation coefficients between the IMF B_z and the R-M effect are much higher than

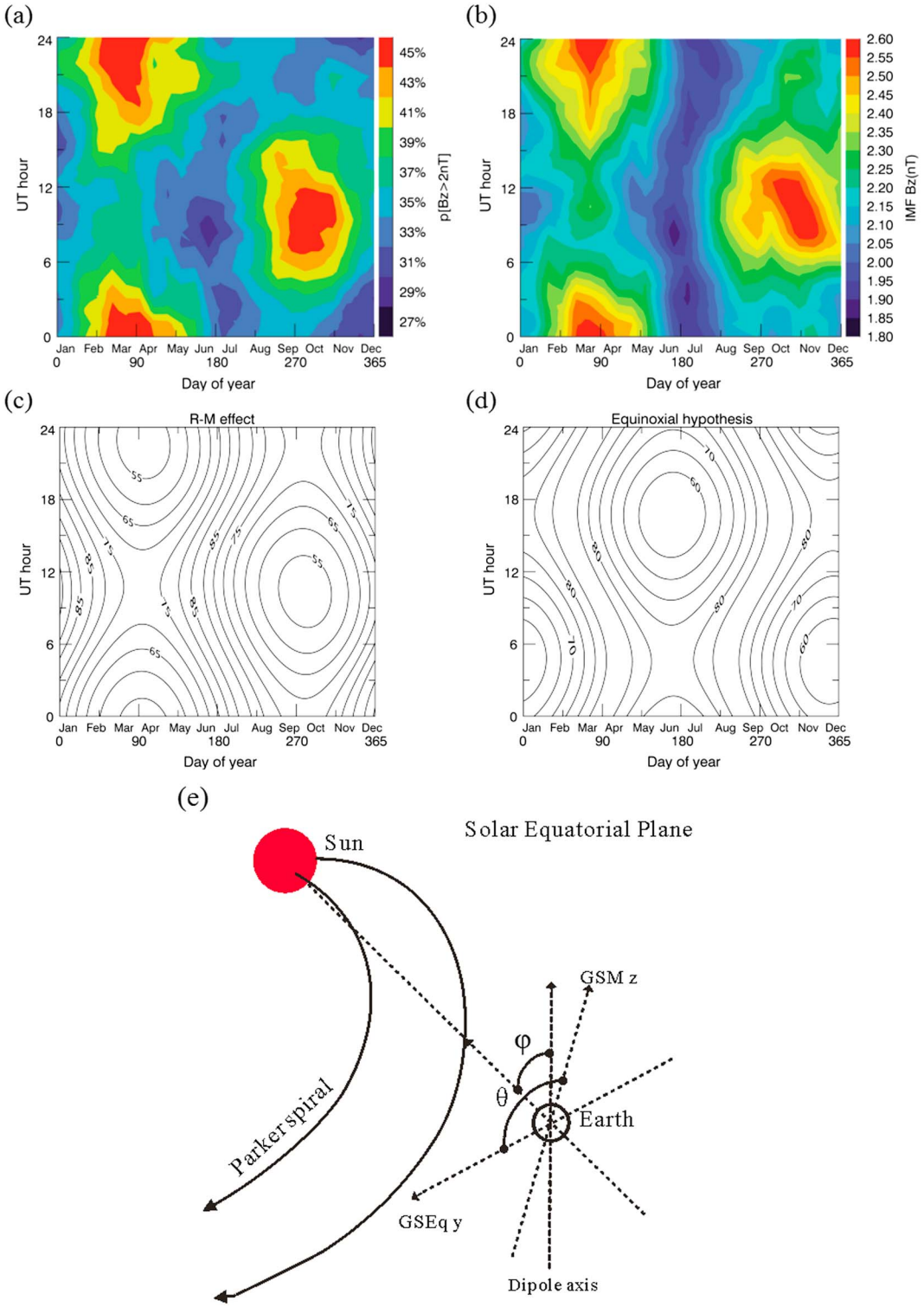

Figure 3. Seasonal and diurnal variations of northward IMF: (a) probability of IMF GSM $B_Z > 2$ nT and (b) the mean value of IMF B_Z. The theoretical calculation of Russell-McPherron effect and the equinoctial hypothesis: (c) seasonal and diurnal variations of θ angle between Z axis in GSM coordinate system and Y axis in GSE coordinate system, (d) seasonal and diurnal variations of φ angle between Earth-Sun line and the dipole axis of the Earth, and (e) the schematic diagram of θ angle for R-M effect and φ angle for equinotical hypothesis.

Table 1
Summarization of Correlation Coefficients Between the Northward IMF B_z and Two Hypothesis

Correlation coefficient	Probability of IMF $B_z > 2$ nT	Mean value of IMF B_z (nT)
R-M effect	0.83	0.84
Equinoctial hypothesis	0.32	0.34

those calculated between the IMF B_z and equinoctial hypothesis. Therefore, we suggest that the R-M effect is a more probable hypothesis to explain the seasonal and diurnal northward IMF variations shown in Figure 3 than the equinoctial hypothesis. According to the diurnal variation of the IMF B_z shown in Figures 3a–3c, the period of high probability of the higher northward IMF should be larger in March and September, and therefore, it is likely that there will be long periods of northward IMF during the 2 months. Since the formation of CDPS is related to the long duration of periods of northward IMF and the increased positive B_z magnitude, we consider that the semiannual variation of CDPS occurrence is also related to R-M effect.

3. Summary and Discussion

In this paper, we have performed a statistical analysis of the occurrence of the CDPS and the magnitude of the northward IMF B_z. We find 636 CDPS events and 3,770 PS events, and the CDPS occurrence on the dawnside is slightly higher than that on the duskside, but the difference is not significant. Based on direct in situ observations, a clear dawn-dusk asymmetry of ion density within CDPS events is shown and this dawn-dusk asymmetry is not reflected in spatial distribution of ion temperatures. This indicates that the transport of CDPS events from the flanks to the central magnetotail is more efficient on the dawnside, which confirms previous works from indirect observations (e.g., Wing et al., 2005; Wing & Newell, 2002). Most of the CDPS events that we observed are during geomagnetic quiet times ($Kp < 3$, $AE < 150$ nT; see Figure S2) and experience a long duration of northward IMF prior to the event. The occurrence rate of CDPS shows a semiannual variation. This variation of CDPS occurrence is still clear using a subset of CDPS events with long intervals of northward IMF. Using the OMNI data set, we investigate the seasonal and diurnal variations of the magnitude of the IMF B_z under northward IMF conditions. The magnitude of IMF B_z peaks at spring and fall equinoxes and reaches the minimum at summer and winter solstices. The seasonal and diurnal variations of IMF B_z are more consistent with the R-M effect than the equinoctial hypothesis.

The equinoctial hypothesis could also affect the CDPS occurrence by affecting the threshold of shear flow velocity (Boller & Stolov, 1970) and lead to a semiannual variation of CDPS occurrences. If the equinoctial hypothesis is more important, the dawn-dusk asymmetry of CDPS occurrence could be expected due to the dawn-dusk asymmetry of K-H instability (e.g., Nykyri, 2013). However, the difference between the duskside and dawnside in our CDPS occurrence is not so significant, and both K-H instability and the high-latitude reconnection are easier to occur when the magnitude of IMF B_z is larger during northward IMF intervals. The long duration of northward IMF, which is often observed before the CDPS events, appears to be more likely to occur in March and September than in June and December. The axial hypothesis suggests that the variation of the average solar wind velocity is a key factor in the semiannual variation of geomagnetic activity during active times, but the CDPS events we observed are during quiet times, and not related to the solar wind entry under southward IMF conditions. We therefore suggest that both the equinoctial hypothesis and the R-M effect create better conditions than axial hypothesis for solar wind entry under northward IMF conditions in March and September. Of these two alternatives, our statistical study of IMF B_z occurrence probability is consistent with the R-M effect, and clearly inconsistent with the equinoctial hypothesis. As a result, the cold and dense plasma sheet should be easier to form, which explains the higher occurrence rate of CDPS observed during spring and fall equinoxes. The CDPS is a critical component of storm time ring current dynamics (Chen et al., 2007; Lavraud, Thomsen, Borovsky, et al., 2006; Thomsen et al., 2003) and magnetosphere-ionosphere coupling (e.g., Gkioulidou et al., 2009). Here we show that the CDPS has a seasonal dependence, which in turn will be reflected in both the formation and generation of the ring current and more generally, magnetosphere-ionosphere coupling.

Acknowledgments
We acknowledge use of OMNI data obtained from OMNIWeb service at http://omniweb.gsfc.nasa.gov The Geotail/MGF, Geotail/LEP, and Geotail/CPI data were provided via www.darts.isas.jaxa.jp/stp/geotail/. This work was supported by the National Natural Science Foundation of China (grant 41574157, 41628402, and 41774153), the Shandong University (Weihai) Future Plan for Young Scholar (2017WHWLJH08),and the SNSB grant 77/14. A.N.F. is funded in part by STFC grant ST/N00722/1, and I.J.R. is funded in part by STFC grant ST/N00722/1 and NERC grants NE/L007495/1, NE/P017150/1, and NE/P017185/1.

References

Bartels, J. (1932). Terrestrial-magnetic activity and its relations to solar phenomena. *Journal of Geophysical Research*, *37*(1), 1–52. https://doi.org/10.1029/TE037i001p00001

Baumjohann, W., Paschmann, G., & Cattell, C. A. (1989). Average plasma properties in the central plasma sheet. *Journal of Geophysical Research*, *94*(A6), 6597–6606. https://doi.org/10.1029/JA094ia06p06597

Boller, B. R., & Stolov, H. L. (1970). Kelvin-Helmholtz instability and the semiannual variation of geomagnetic activity. *Journal of Geophysical Research*, *75*(31), 6073–6084. https://doi.org/10.1029/JA075i031p06073

Borovsky, J. E., Thomsen, M. F., & Elphic, R. C. (1998). The driving of the plasma sheet by the solar wind. *Journal of Geophysical Research*, *103*(A8), 17,617–17,639. https://doi.org/10.1029/97JA02986

Chen, M. W., Wang, C., Schulz, M., & Lyons, L. R. (2007). Solar-wind influence on mlt dependence of plasma sheet conditions and their effects on storm time ring current formation. *Geophysical Research Letters*, *34*, L14112. https://doi.org/10.1029/2007GL030189

Cliver, E. W., Kamide, Y., & Ling, A. G. (2000). Mountains versus valleys: Semiannual variation of geomagnetic activity. *Journal of Geophysical Research*, *105*(A2), 2413–2424. https://doi.org/10.1029/1999JA900439

Cliver, E. W., Kamide, Y., & Ling, A. G. (2002). The semiannual variation of geomagnetic activity: Phases and profiles for 130 years of aa, data. *Journal of Atmospheric and Solar-Terrestrial Physics*, *64*(1), 47–53. https://doi.org/10.1016/s1364-6826(01)00093-1

Cortie, A. L. (1912). Sunspots and terrestrial magnetic phenomena, 1898–1911. *Monthly Notices of the Royal Astronomical Society*, *73*(3), 148–155. https://doi.org/10.1093/mnras/73.3.148/

Crooker, N. U. (1992). Reverse convection. *Journal of Geophysical Research*, *97*(A12), 19,363. https://doi.org/10.1029/92JA01532

Crooker, N. U., & Siscoe, G. L. (1986). On the limits of energy-transfer through dayside merging. *Journal of Geophysical Research*, *91*(A12), 3393–3397. https://doi.org/10.1029/JA091ia12p13393

Echim, M., & Lemaire, J. (2002). Positive density gradients at the magnetopause: Interpretation in the framework of the impulsive penetration mechanism. *Journal of Atmospheric and Solar-Terrestrial Physics*, *64*(18), 2019–2028. https://doi.org/10.1016/s1364-6826(02)00229-8

Fairfield, D. H., Otto, A., Mukai, T., Kokubun, S., Lepping, R. P., Steinberg, J. T., … Yamamoto, T. (2000). Geotail observations of the Kelvin-Helmholtz instability at the equatorial magnetotail boundary for parallel northward fields. *Journal of Geophysical Research*, *105*(A9), 21,159–21,173. https://doi.org/10.1029/1999JA000316

Frank, L. A., Ackerson, K. L., Paterson, W. R., Lee, J. A., English, M. R., & Pickett, G. L. (1994). The Comprehensive Plasma Instrumentation (CPI) for the Geotail spacecraft. *Journal of Geomagnetism and Geoelectricity*, *46*(1), 23–37. https://doi.org/10.5636/jgg.46.23

Fujimoto, M., Mukai, T., & Kokubun, S. (2002). Cold-dense plasma sheet and hot-dense ions in the inner-magnetosphere. *Advances in Global Magnetospheric Structure, Dynamics, and Region Coupling, Proceedings*, Pii S0273-1177(02)00700-7, *30*(10), 2279–2288. https://doi.org/10.1016/S0273-1177(02)80246-0

Fujimoto, M., Nishida, A., Mukai, T., Saito, Y., Yamamoto, T., & Kokubun, S. (1996). Plasma entry from the franks of the near-Earth magnetotail: GEOTAIL observations in the dawnside LLBL and the plasma sheet. *Journal of Geomagnetism and Geoelectricity*, *48*(5), 711–727. https://doi.org/10.5636/jgg.48.711

Fujimoto, M., Tonooka, T., & Mukai, T. (2003). Vortex-like fluctuations in the magnetotail flanks and their possible roles in plasma transport. In P. T. Newell & T. Onsager (Eds.), *Earth's low-latitude boundary layer* (pp. 241–251). Washington, DC: American Geophysical Union. https://doi.org/10.1029/133GM24

Fuselier, S. A. Jr., Waite, J. H., Avanov, L. A., Smirnov, V. M., Vaisberg, O. L., Siscoe, G., & Russell, C. T. (2002). Characteristics of magnetosheath plasma in the vicinity of the high-altitude cusp. *Planetary and Space Science*, *50*(5–6), 559–566. https://doi.org/10.1016/s0032-0633(02)00035-1

Gkioulidou, M., Wang, C. P., Lyons, L. R., & Wolf, R. A. (2009). Formation of the harang reversal and its dependence on plasma sheet conditions: Rice convection model simulations. *Journal of Geophysical Research*, *114*, A07204. https://doi.org/10.1029/2008JA013955

Hasegawa, H., Fujimoto, M., Phan, T.-D., Rème, H., Balogh, A., Dunlop, M. W., … TanDokoro, R. (2004). Transport of solar wind into Earth's magnetosphere through rolled-up Kelvin-Helmholtz vortices. *Nature*, *430*(7001), 755–758. https://doi.org/10.1038/nature02799

Hasegawa, H., Retinò, A., Vaivads, A., Khotyaintsev, Y., André, M., Nakamura, T. K. M., … Canu, C. (2009). Kelvin-Helmholtz waves at the Earth's magnetopause: Multiscale development and associated reconnection. *Journal of Geophysical Research*, *114*, A12207. https://doi.org/10.1029/2009JA014042

Hundhausen, A. J., Bame, S. J., & Montgomery, M. D. (1971). Variations of solar-wind plasma properties: Vela observations of a possible heliographiclatitude-dependence. *Journal of Geophysical Research*, *76*(22), 5145–5154. https://doi.org/10.1029/JA076i022p05145

Kokubun, S., Yamamoto, T., Acuna, M. H., Hayashi, K., Shiokawa, K., & Kawano, H. (1994). The Geotail magnetic-field experiment. *Journal of Geomagnetism and Geoelectricity*, *46*(1), 7–21. https://doi.org/10.5636/jgg.46.7

Lavraud, B., Thomsen, M. F., Borovsky, J. E., Denton, M. H., & Pulkkinen, T. I. (2006). Magnetosphere preconditioning under northward IMF: Evidence from the study of coronal mass ejection and corotating interaction region geoeffectiveness. *Journal of Geophysical Research*, *111*, A09208. https://doi.org/10.1029/2005JA011566

Lavraud, B., Thomsen, M. F., Lefebvre, B., Schwartz, S. J., Seki, K., Phan, T. D., … Balogh, A. (2006). Evidence for newly closed magnetosheath field lines at the dayside magnetopause under northward IMF. *Journal of Geophysical Research*, *111*, A05211. https://doi.org/10.1029/2005JA011266

Lavraud, B., Thomsen, M. F., Taylor, M. G. G. T., Wang, Y. L., Phan, T. D., Schwartz, S. J., … Balogh, A. (2005). Characteristics of the magnetosheath electron boundary layer under northward interplanetary magnetic field: Implications for high-latitude reconnection. *Journal of Geophysical Research*, *110*, A06209. https://doi.org/10.1029/2004JA010808

Le, G., Russell, C. T., Gosling, J. T., & Thomsen, M. F. (1996). ISEE observations of low-latitude boundary layer for northward interplanetary magnetic field: Implications for cusp reconnection. *Journal of Geophysical Research*, *101*(A12), 27,239–27,249. https://doi.org/10.1029/96JA02528

Li, W. H., Raeder, J., Dorelli, J., Oieroset, M., & Phan, T. D. (2005). Plasma sheet formation during long period of northward IMF. *Geophysical Research Letters*, *32*, L12S08. https://doi.org/10.1029/2004GL021524

Li, W. H., Raeder, J., Thomsen, M. F., & Lavraud, B. (2008). Solar wind plasma entry into the magnetosphere under northward IMF conditions. *Journal of Geophysical Research*, *113*, A04204. https://doi.org/10.1029/2007JA012604

Lin, D., Wang, C., Li, W. Y., Tang, B. B., Guo, X. C., & Peng, Z. (2014). Properties of Kelvin-Helmholtz waves at themagnetopause under northward interplanetary magnetic field: Statistical study. *Journal of Geophysical Research: Space Physics*, *119*, 7485–7494. https://doi.org/10.1002/2014JA020379

McIntosh, D. H. (1959). On the annual variation of magnetic disturbance. *Philosophical Transactions of the Royal Society A: Mathematical, Physical and Engineering Sciences*, *251*(1001), 525–552. https://doi.org/10.1098/rsta.1959.0010

Miura, A. (1987). Simulation of Kelvin-Helmholtz instability at the magnetospheric boundary. *Journal of Geophysical Research*, *92*(A4), 3195–3206. https://doi.org/10.1029/JA092iA04p03195

Mukai, T., Machida, S., Saito, Y., Hirahara, M., Terasawa, T., Kaya, N., … Nishida, A. (1994). The Low-Energy Particle (LEP) experiment onboard the Geotail satellite (Vol 46, Pg 669, 1994). *Journal of Geomagnetism and Geoelectricity*, *46*(10), 909–909. https://doi.org/10.5636/jgg.46.669

Nishino, M. N., Fujimoto, M., Terasawa, T., Ueno, G., Maezawa, K., Mukai, T., & Saito, Y. (2007a). Geotail observations of temperature anisotropy of the two-component protons in the dusk plasma sheet. *Annales Geophysicae*, *25*(3), 769–777. https://doi.org/10.5194/angeo-25-769-2007

Nishino, M. N., Fujimoto, M., Terasawa, T., Ueno, G., Maezawa, K., Mukai, T., & Saito, Y. (2007b). Temperature anisotropies of electrons and two-component protons in the dusk plasma sheet. *Annales Geophysicae*, *25*(6), 1417–1432. https://doi.org/10.5194/angeo-25-1417-2007

Nishino, M. N., Fujimoto, M., Ueno, G., Maezawa, K., Mukai, T., & Saito, Y. (2007). Geotail observations of two-component protons in the midnight plasma sheet. *Annales Geophysicae*, *25*(10), 2229–2245. https://doi.org/10.5194/angeo-25-2229-2007

Nishino, M. N., Fujimoto, M., Ueno, G., Mukai, T., & Saito, Y. (2007). Origin of temperature anisotropies in the cold plasma sheet: Geotail observations around the Kelvin-Helmholtz vortices. *Annales Geophysicae*, *25*(9), 2069–2086. https://doi.org/10.5194/angeo-25-2069-2007

Nowada, M., Shue, J. -H., & Russell, C. T. (2009). Effects of dipole tilt angle on geomagnetic activity. *Planetary and Space Science*, *57*, 1254–1259. https://doi.org/10.1016/j.pss.2009.04.007

Nykyri, K. (2013). Impact of MHD shock physics on magnetosheath asymmetry and Kelvin-Helmholtz instability. *Journal of Geophysical Research: Space Physics*, *118*, 5068–5081. https://doi.org/10.1002/jgra.50499

O'Brien, T. P., & McPherron, R. L. (2002). Seasonal and diurnal variationof Dst dynamics. *Journal of Geophysical Research*, *107*(A11), 1341. https://doi.org/10.1029/2002JA009435

Olson, W. P., & Pfitzer, K. A. (1985). Magnetospheric responses to the gradient drift entry of solar wind plasma. *Journal of Geophysical Research*, *90*(A11), 10,823–10,833. https://doi.org/10.1029/JA090iA11p10823

Onsager, T. G., Scudder, J. D., Lockwood, M., & Russell, C. T. (2001). Reconnection at the high-latitude magnetopause during northward interplanetary magnetic field conditions. *Journal of Geophysical Research*, *106*(A11), 25,467–25,488. https://doi.org/10.1029/2000JA000444

Russell, C. T., & McPherron, R. L. (1973). Semiannual variation of geomagnetic activity. *Journal of Geophysical Research*, *78*(1), 92–108. https://doi.org/10.1029/JA078i001p00092

Russell, C. T., Wang, Y. L., & Raeder, J. (2003). Possible dipole tilt dependence of dayside magnetopause reconnection. *Geophysical Research Letters*, *30*(18), 1937. https://doi.org/10.1029/2003GL017725

Sabine, E. (1851). On periodical laws discoverable in the mean effects of the larger magnetic disturbances. *Philosophical Transactions of the Royal Society of London*, *141*, 123–139. https://doi.org/10.1098/rspl.1856.0011

Sandholt, P. E., Farrugia, C. J., Cowley, S. W. H., Denig, W. F., Lester, M., Moen, J., & Lybekk, B. (1999). Capture of magnetosheath plasma by the magnetosphere during northward IMF. *Geophysical Research Letters*, *26*(18), 2833–2836. https://doi.org/10.1029/1999GL900600

Sharma, A. S., Nakamura, R., Runov, A., Grigorenko, E. E., Hasegawa, H., Hoshino, M., … Snekvik, K. (2008). Transient and localized processes in the magnetotail: A review. *Annales Geophysicae*, *26*(4), 955–1006. https://doi.org/10.5194/angeo-26-955-2008

Shi, Q. Q., Zong, Q. G., Fu, S. Y., Dunlop, M. W., Pu, Z. Y., Parks, G. K., … Lucek, E. (2013). Solar wind entry into the high-latitude terrestrial magnetosphere during geomagnetically quiet times. *Nature Communications*, *4*, 1466. https://doi.org/10.1038/Ncomms2476

Shi, Q. Q., Zong, Q. G., Zhang, H., Pu, Z. Y., Fu, S. Y., Xie, L., … Lucek, E. (2009). Cluster observations of the entry layer equatorward of the cusp under northward interplanetary magnetic field. *Journal of Geophysical Research*, *114*, A12219. https://doi.org/10.1029/2009JA014475

Shue, J. H., Song, P., Russell, C. T., Steinberg, J. T., Chao, J. K., Zastenker, G., … Kawano, H. (1998). Magnetopause location under extreme solar wind conditions. *Journal of Geophysical Research*, *103*(A8), 17,691–17,700. https://doi.org/10.1029/98JA01103

Siscoe, G., & Crooker, N. (1996). Diurnal oscillation of Dst: A manifestation of the Russell-McPherron effect. *Journal of Geophysical Research*, *101*(A11), 24,985–24,989. https://doi.org/10.1029/96JA01875

Song, P., & Russell, C. T. (1992). Model of the formation of the low-latitude boundary layer for strongly northward interplanetary magnetic field. *Journal of Geophysical Research*, *97*(A2), 1411. https://doi.org/10.1029/91JA02377

Stenuit, H, Fujimoto, M., Fuselier, S. A., Sauvaud, J.-A., Wing, S., Fedorov, A., … Pedersen, A. (2002). Multi-spacecraft study ion the dynamics of the dusk-flank magnetosphere under northward IMF: January 10–11, 1997. *Journal of Geophysical Research 107*(A10), 1333. https://doi.org/10.1029/2002JA9009246

Svalgaard, L. (1977). Geomagnetic activity: Dependence on solar wind parameters. In J. B. Zirker (Ed.), *Coronal holes and high speed wind streams* (pp. 371). Boulder, CO: Colorado Association University Press.

Terasawa, T., Fujimoto, M., Mukai, T., Shinohara, I., Saito, Y., Yamamoto, T., … Lepping, R. P. (1997). Solar wind control of density and temperature in the near- Earth plasma sheet: WIND/GEOTAIL collaboration. *Geophysical Research Letters*, *24*(8), 935–938. https://doi.org/10.1029/96GL04018

Thomsen, M. F., Borovsky, J. E., Skoug, R. M., & Smith, C. W. (2003). Delivery of cold, dense plasma sheet material into the near-Earth region. *Journal of Geophysical Research*, *108*(A4), 1151. https://doi.org/10.1029/2002JA009544

Wang, C.-P., Gkioulidou, M., Lyons, L. R., Xing, X., & Wolf, R. A. (2014). Interchange motion as a transport mechanism for formation of cold-dense plasma sheet. *Journal of Geophysical Research: Space Physics*, *119*, 8318–8337. https://doi.org/10.1002/2014JA020251

Wing, S., Johnson, J. R., & Fujimoto, M. (2006). Timescale for the formation of the cold-dense plasma sheet: A case study. *Geophysical Research Letters*, *33*, L23106. https://doi.org/10.1029/2006GL027110

Wing, S., Johnson, J. R., Newell, P. T., & Meng, C.-I. (2005). Dawn-dusk asymmetries, ion spectra, and sources in the northward interplanetary magnetic field plasma sheet. *Journal of Geophysical Research*, *110*, A08205. https://doi.org/10.1029/2005JA011086

Wing, S., & Newell, P. T. (2002). 2D plasma sheet ion density and temperature profiles for northward and southward IMF. *Geophysical Research Letters*, *29*(9), 1307. https://doi.org/10.1029/2001GL013950

Zhao, H., & Zong, Q. G. (2012). Seasonal and diurnal variation of geomagnetic activity: Russell-McPherron effect during different IMF polarity and/or extreme solar wind conditions. *Journal of Geophysical Research*, *117*, A11222. https://doi.org/10.1029/2012JA017845

Zhou, X.-Z., Pu, Z. Y., Zong, Q.-G., & Xie, L. (2007). Energy filter effect for solar wind particle entry to the plasma sheet via flank regions during southward interplanetary magnetic field. *Journal of Geophysical Research*, *112*, A06233. https://doi.org/10.1029/2006JA012180